Available online at www.sciencedirect.com
ScienceDirect
Building and Environment 42 (2007) 866–876
BUILDING AND ENVIRONMENT
www.elsevier.com/locate/buildenv

# Defining standard skies for Hong Kong

Edward Ng*, Vicky Cheng, Ankur Gadi, Jun Mu, Max Lee, Ankit Gadi

*Department of Architecture, The Chinese University of Hong Kong, Shatin, New Territories, Hong Kong SAR, China*

Received 19 July 2005; received in revised form 26 August 2005; accepted 12 October 2005

**Abstract**

A CIE International Daylight Monitoring Programme (IDMP) general class station was established in 2000 at the Chinese University of Hong Kong. The station was upgraded to Research Class IDMP Station in April 2003. The study, which includes the sky luminance scan data collected from April 2003 to May 2005, firstly fits the data to the CIE Standard General Sky definitions, which consist of 15 luminance distributions for modeling the sky from the heavily overcast sky to cloudless clear sky. Then the paper proposes a reduced set of CIE general skies (and their probability of occurrence) to represent the sky conditions of Hong Kong. This reduced set will be known in this paper as "Hong Kong Representative Sky" (HKRS). Further, the paper evaluates the sensitivity of vertical sky component (VSC) to differences between the HKRS and the standard CIE Overcast Sky model. Comparing with observed data, it is demonstrated that the HKRS could give better results. A reduction in error of approximately 20–40% could be expected, depending on the orientation of a surface. Using the HKRS, building designers could better predict daylight availability of their design. Energy saving and more sustainable buildings might result.


*Keywords:* CIE general standard sky; Hong Kong representative sky; Vertical sky component

## 1. Background

Hong Kong lies along the southern coast of China with latitude of 22.3°N and longitude of 114.2°E. It is a hilly land with many islands situated beside the South China Sea. Hong Kong's climate is sub-tropical, tending towards temperate for nearly half the year.

### 1.1. Measuring station

The CIE IDMP Research Class measuring station is located on the top of a water tower 30 m above ground level (approximately 150 m above sea level) in the Chinese University of Hong Kong, as shown in Fig. 1. Within a 5 km radius of the station, 55% of the land is hills and natural landscape, 25% is the sea area, 20% is the build up, and there is a main highway and railway line around 0.6 km east of the measurement site. The site is relatively free from external obstruction, heavy pollution, and conforms to site specification in the CIE Guide to Daylight Measurement. (CIE Guideline (CIE 108-1994), [1]).

The instrumentation at the station, as shown in Figs. 2(a) and (b), consists of six photometers and two pyranometers for horizontal solar radiation and daylight illuminance data measurements. The global horizontal illuminance ($E_{vg}$) was measured with an EKO luxmeter (ML-020S-O) and the global horizontal irradiance ($E_{eg}$) is measured using EKO pyranometer (MS-64). The diffuse luxmeter (and pyranometer) is obscured from the direct sun by a Shadow Ball. Four illuminance sensors are installed in a vertical mounting base facing to each direction of North, East, South and West. The direct solar illuminance ($E_{vs}$) sensor is installed in the Sun Tracker facing to the sun.

A General Class Station was established in 2000. The station was upgraded to Research Class IDMP Station in April 2003. The sky luminance distribution data were measured with an EKO sky scanner (MS-321LR). The study included the sky luminance scan data collected from April 2003 to May 2005, but excluded the period during September 2003–October 2003 and 15 November

*Corresponding author. Tel.: +852 2609 6515; fax: +852 2603 5267.
*E-mail address:* edwardng@cuhk.edu.hk (E. Ng).

0360-1323/$ - see front matter 
doi:10.1016/j.buildenv.2005.10.005

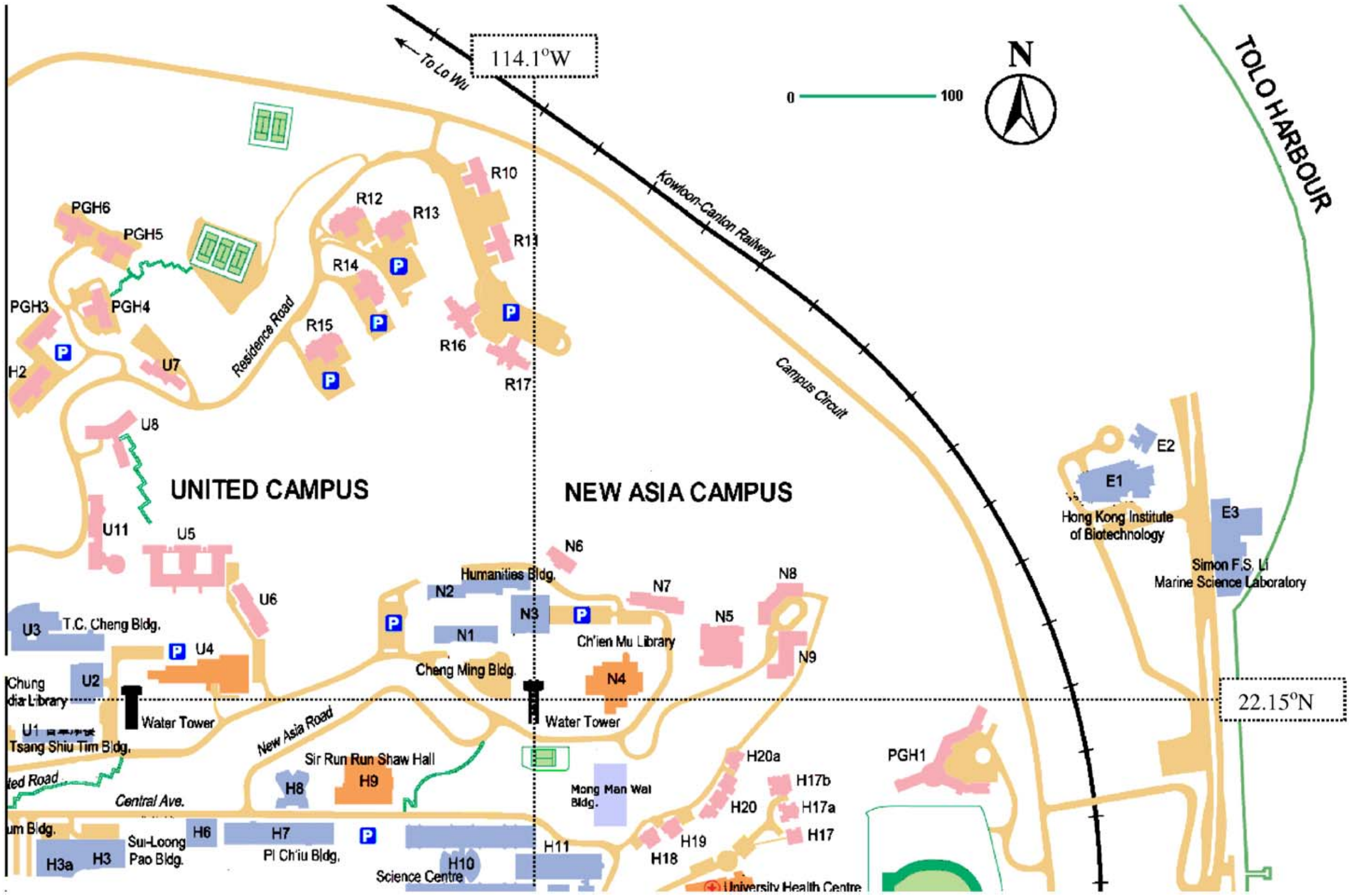


Fig. 1. Location of the IDMP station at CUHK.

2004–December 2004 when the instrument malfunctioned and was sent back to the manufacturer for repair.

The sky scanner measures luminance of 145 points of sky hemisphere but it does not record luminance data greater than 50 kcd/m$^2$. The sky luminance scan data were taken every 10 min. The data analyzed in this study consist of 24,000 sky scans, and they were obtained after the measured data (approximately 60,000 data points) was quality controlled based on CIE Guide to Daylight Measurement (CIE Guideline (CIE 108-1994), [1]). These data points are presented in Fig. 3.

## 2. Introduction

The use of daylight in buildings provides a better and a welcoming ambience. It leads to reducing the energy consumed by electric lighting, and hence to cutting atmospheric pollution. It also leads to improved health and productivity (Boyce [2]).

Design for day lighting is of growing concerns. In the lack of a definite reference of sky conditions, day lighting calculation procedures and lighting simulation software are currently based on the CIE Standard Overcast Sky (Compte Rendu CIE 12 Session, [3]), which was defined in the early 1950s. However, the standard overcast sky does not generally truly represent the actual sky conditions of Hong Kong or indeed anywhere else on Earth. New models of sky representations of Hong Kong's sky conditions maybe beneficial in predicting daylight availability.

This paper presents the result of sky luminance scans collected in a research-class CIE IDMP station at the Chinese University of Hong Kong. The paper proposes a reduced set of CIE general skies to represent the sky conditions of Hong Kong. The paper is inspired by Tregenza [4], and the main methodology is based on Tregenza [5]. The paper also evaluates the sensitivity of vertical sky component to differences between proposed new skies and the standard CIE Overcast Sky model. The proposed set of standard skies and their probability of occurrence can become a reference for daylighting calculation and energy simulation of buildings in Hong Kong.

## 3. CIE standard sky models

The luminance pattern of the sky depends on location, weather and climate, and it changes during the day and with the position of the sun. The CIE Standard General Sky defines a set of luminance distributions, which model the sky under a wide range of conditions, from the heavily overcast sky to cloudless clear sky (CIE Standard (CIE S

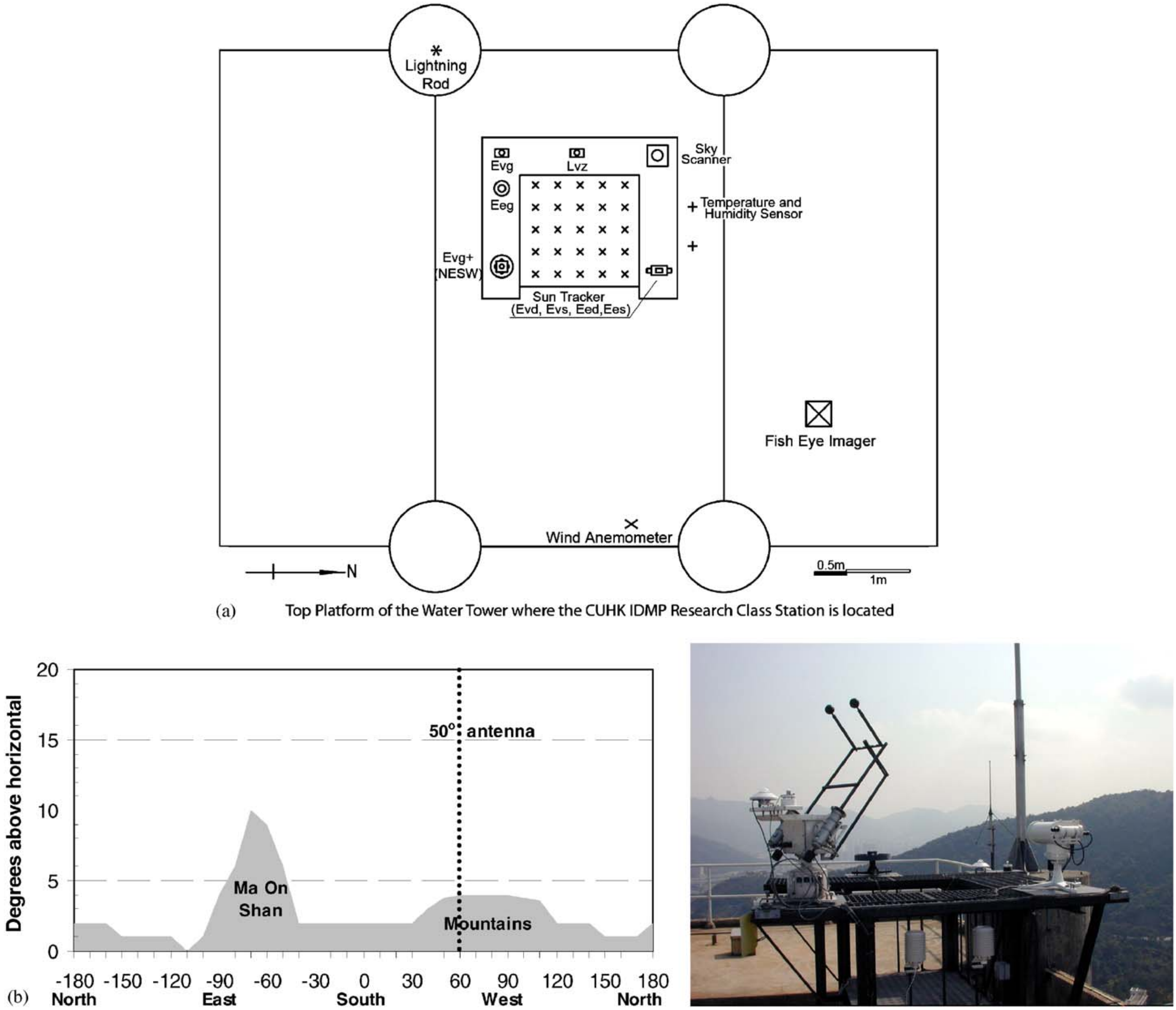


Fig. 2. (a) Detailed set up of the IDMP station at CUHK, (b) Obstructions for global horizontal illuminance sensor and a picture of the station.

011/E:2003 [6]). The luminance distributions are given in two functions: $\varphi(Z)$, the gradation function, which describes the luminance gradation between horizon and zenith; and $f(\chi)$, the relative scattering indicatrix, which relates sky luminance with angular distance from the sun. The relative luminance $(L/L_z)$ at any point in the sky is defined as follows:

$$\frac{L}{L_z} = \frac{f(\chi)\varphi(Z)}{f(Z_s)\varphi(0)}, \tag{1}$$

where $L$ is the luminance of a sky element (cd/m$^2$), $L_z$ the zenith luminance (cd/m$^2$), $\chi$: the angular distance between sky element and the sun (radian), $Z$ the zenith angle of sky element (radian) and $Z_s$ the zenith angle of the sun (radian).

The gradation function and the indicatrix function are governed by five adjustable parameters, which in different combinations constitute the 15 standard luminance distributions. Luminance distributions of the 15 standard skies are illustrated in Fig. 4 and the descriptions are given in Table 1.

Tregenza [4] has compared these 15 standard luminance distributions with measured luminance distributions from four stations–Singapore (1.5°N, 104°E), Fukuoka (Japan 33.5°N, 130°E), Garston (UK 51.7°N, 0.4°W), and Sheffield (UK53.48°N, 1.5°W), which represent tropical humid climate and temperate maritime climate. The results suggested that the standard set of luminance distributions gives a good overall framework for categorizing actual skies and the subsets of four luminance distributions was

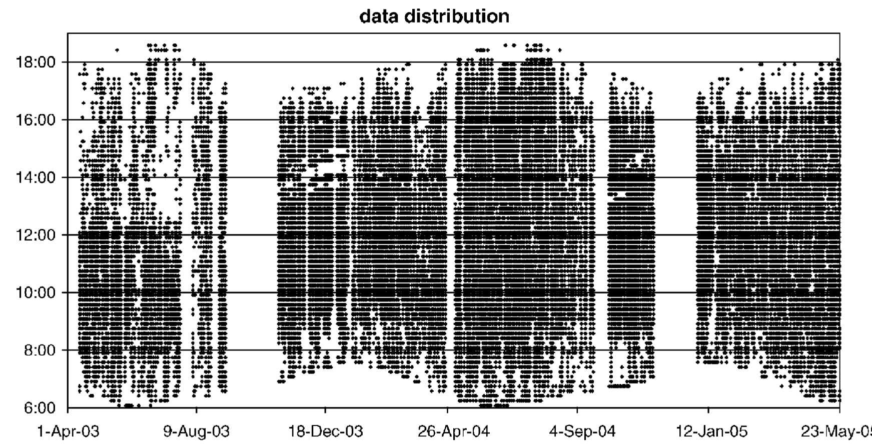


Fig. 3. Data distribution for sky scanner data (after QC—approximately 24,000 data points).

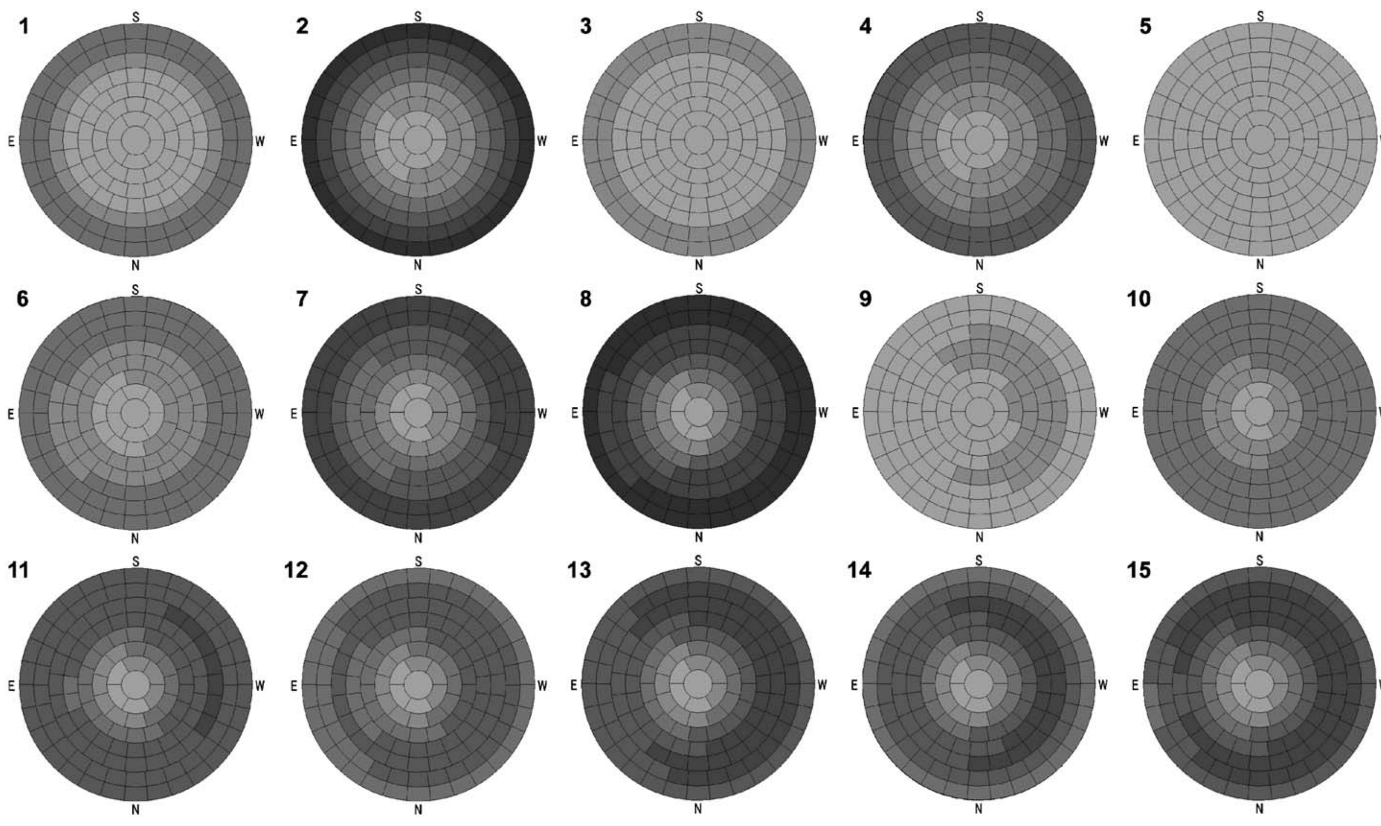


Fig. 4. Luminance distribution of the 15 standard skies in June with solar altitude 85° and azimuth N80°E.

adequate to describe the skies that occurred at each site (Tregenza [4]).

Li et al. [7] have collected sky luminance data of Hong Kong for 3 years from January 1999 to December 2001. They studied the measured data against the 15 standard luminance distributions and concluded that a subset of five best-fit standard skies (sky types 1, 3, 6, 11 and 13 with probability of occurrence as 16, 15, 24, 21, 24%, respectively) would be sufficient to describe the sky conditions of Hong Kong without any significant deterioration in the accuracy of prediction (Li et al. [7]). The work of Li et al. [7] represented a significant step towards the identification of daylight climate of Hong Kong. However, the proposed best-fit standard skies were not widely adopted because the implication of using the proposed standard skies in replacing the overcast sky on daylight and energy prediction was not clearly known. To evaluate the implication of the new sky model on daylight prediction and to verify the findings of Li et al. [7], study of Hong Kong sky conditions was repeated and extended

Table 1
CIE general sky type description (CIE, 2003)

| Type | Luminance distribution |
|---|---|
| 1 | CIE standard overcast sky, steep luminance gradation towards zenith, azimuthal uniformity |
| 2 | Overcast, with steep luminance gradation and slight brightening towards the sun |
| 3 | Overcast, moderately graded with azimuthal uniformity |
| 4 | Overcast, moderately graded and slight brightening towards the sun |
| 5 | Sky of uniform luminance |
| 6 | Partly cloudy sky, no gradation towards zenith, slight brightening towards the sun |
| 7 | Partly cloudy sky, no gradation towards zenith, brighter circumsolar region |
| 8 | Partly cloudy sky, no gradation towards zenith, distinct solar corona |
| 9 | Partly cloudy, with the obscured sun |
| 10 | Partly cloudy, with brighter circumsolar region |
| 11 | White-blue sky with distinct solar corona |
| 12 | CIE standard clear sky, low luminance turbidity |
| 13 | CIE standard clear sky, polluted atmosphere |
| 14 | Cloudless turbid sky with broad solar corona |
| 15 | White-blue turbid sky with broad solar corona |

using sky luminance scan data collected from an IDMP station at the Chinese University of Hong Kong.

## 4. Towards the Hong Kong representative sky

### 4.1. Method

The approach to finding the best-fit standard distribution to a measured brightness pattern has largely followed the methodology set out by Tregenza [5]. The procedure first normalizes sky scan luminance with respect to horizontal illuminance and does the same for the 15 standard general sky types for the solar angles at the time of each scan. Sky patches surrounding the solar disc that subject to huge measuring error are excluded from calculation. The standard luminance pattern that has the minimum least-squares error over the whole sky is the best-fit standard sky type. Finally, the total root-mean-square errors with different subsets of sky types are calculated and compared. The best-fit sky model refers to the subsets that contain the minimum number of standard skies and with reasonable fit to scanned luminance distribution.

### 4.2. Results

Fig. 5(a) shows the distribution of best-fit standard skies calculated from the total 24,000 sky scans and Fig. 5(b) shows the relative RMS error where a particular sky was the best-fit in comparison to the base case where the complete sets of 15 standard skies were used. Fig. 5(a) characterizes the sky conditions of Hong Kong, which is predominantly cloudy. It is interesting to note that overcast

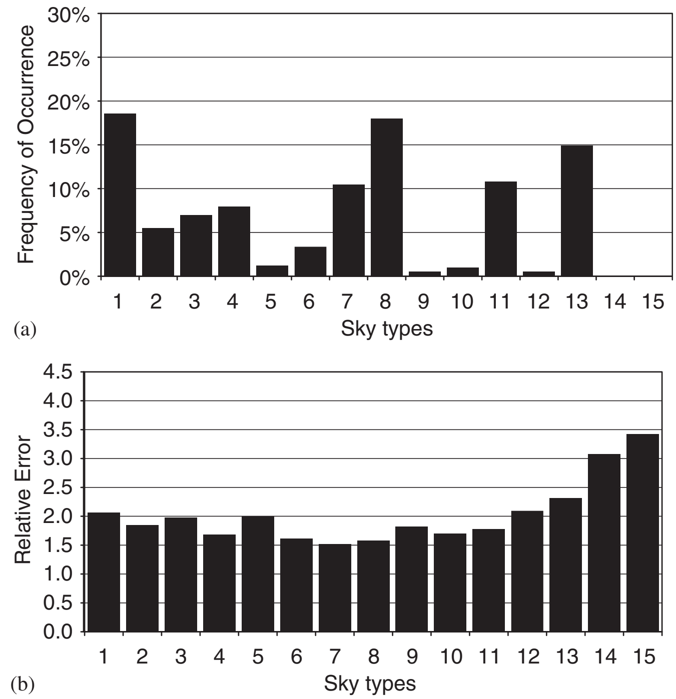


Fig. 5. (a) Frequency distribution of best-fit standard skies, (b) relative RMS error where a particular sky was the best-fit in comparison to the complete set of skies.

(sky types 1–5) to intermediate (sky types 6–10) skies make up about 75% of the time.

Fig. 5(b) indicates the deviation of luminance pattern of each of the 15 standard skies to actual sky condition. The deviation is highest at extreme clear sky (sky type 14 & 15) and smaller in the region of intermediate sky. The distribution of relative error is not related to the frequency of occurrence. For instance, the frequency occurrence of sky type 10 and 11 are very different but their relative errors can be similar. According to Fig. 5(b), the luminance pattern of sky type 7 is, in average, closest to the actual sky condition, though it does not frequently occur during the measurement period.

Some standard skies are rarely applicable or not used at all as seen in Fig. 5(a). Studies conducted by Tregenza [5] and Li et al. [7] suggested that eliminating these skies could simplify the sky model without a significant loss of overall accuracy. Fig. 6(a) shows the total RMS error between standard skies and the measured value against the number of standard skies available in the sky model. The total error does not change much when the number of skies is between three and 15, however when the number of skies is reduced to two, the total error increases rapidly. The graph suggests that subsets of three standard skies are adequate to describe the sky conditions of Hong Kong. Fig. 6(b) shows the frequency distribution of best-fit standard skies with subsets of three sky types.

This subset of three sky types describes ''the representative sky of Hong Kong'' (HKRS), namely this includes sky type 1, 8 and 13, representing the overcast, intermediate and clear sky, respectively. Fig. 7 consists of fisheye photos that show the three corresponding sky conditions in Hong Kong.

### 4.2.1. Seasonal trends in sky types

For the purpose of this study, the 24,000 sky luminance scans were divided into two seasons, summer and winter. The months from April to October spanned summer and from November to March spanned winter, respectively. The analysis was carried out over the winter and summer months of 2003 to 2005. Fig. 8 shows the frequency distribution of best-fit standard skies in summer and winter periods. The analysis over the two seasons suggests an existence of seasonal trend in sky conditions. If one were to bundle sky types 1 to 10 as "generally cloudy" and sky types 11–15 as "clear", then one could clearly see that there are more "clear" skies in the winter as compared to the summer.

The result has important implications when the seasonal data is further analyzed. Table 2 presents a summary of the subsets of best-fit standard skies in the two seasons. There is a significant difference in sky types when the yearly analysis is compared to the seasonal analysis. In summer, the representative sky consists of sky types 1, 4, 8, implying that summer in Hong Kong is generally cloudy to intermediate. While in winter, the representative sky

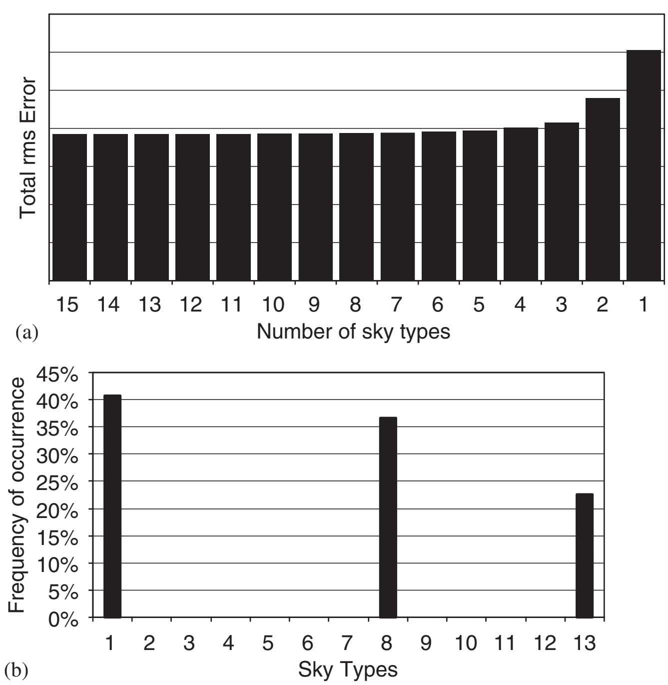


Fig. 6. (a) Total RMS error against number of sky types available, (b) frequency distribution of three best-fit standard skies.

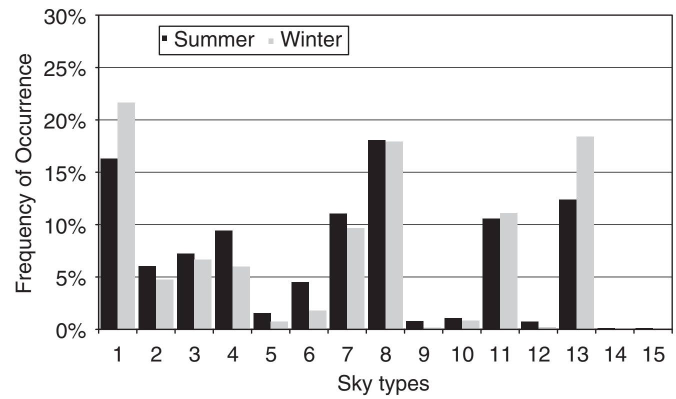


Fig. 8. Seasonal distribution of best-fit standard skies.

Table 2
Subsets of best-fit skies

| Period | Number of sky types | Subsets of best-fit skies | Total RMS error (%) |
|---|---|---|---|
| All data | 3 | 1,8,13 | 21 |
| | 2 | 1,8 | 24 |
| | 1 | 8 | 30 |
| Summer | 3 | 1,4,8 | 18 |
| | 2 | 1,8 | 18 |
| | 1 | 8 | 23 |
| Winter | 3 | 1,8,13 | 13 |
| | 2 | 1,8 | 15 |
| | 1 | 8 | 20 |

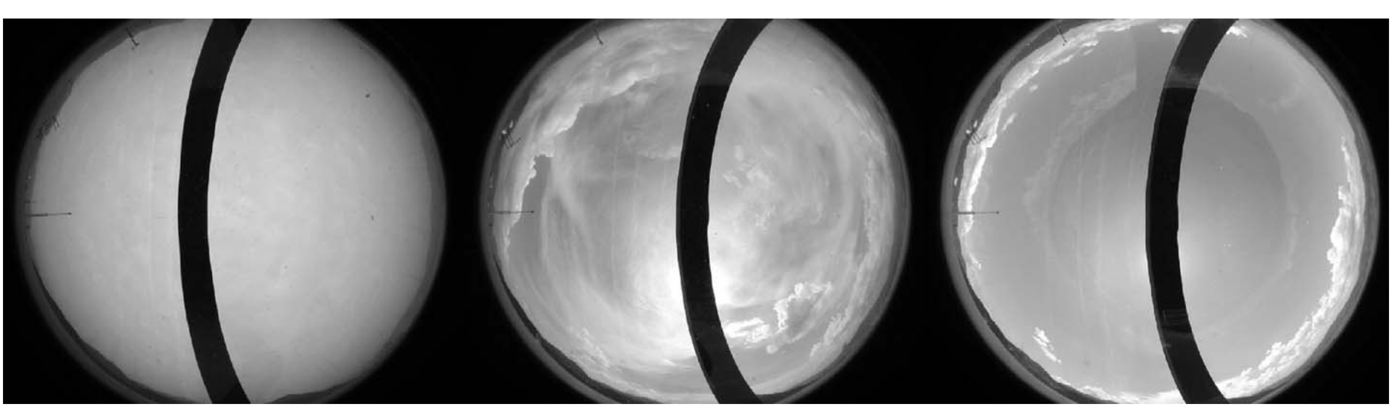

Fig. 7. Fisheye photos of three typical sky conditions in Hong Kong: (left) overcast (sky 1) (middle) intermediate (sky 8) (right) clear (sky 13).

Table 3
Recommended sky types and the frequency

| Period | Number of sky types | Frequency (%) |
|---|---|---|
| All data | 1 | 41 |
| | 8 | 37 |
| | 13 | 22 |
| Summer | 1 | 26 |
| | 4 | 26 |
| | 8 | 48 |
| Winter | 1 | 39 |
| | 8 | 36 |
| | 13 | 25 |

consists of sky types 1, 8, 13, thus implying the presence of more "sunny periods" in the season—this is supported by Fig. 8. Lastly, it is important to notice that seasonal analysis can lead to a significant reduction in total error in both summer and winter, as shown in Table 2.

Table 3 provides a summary of the recommended sky types (with their frequency distribution) for Hong Kong sky conditions.

## 5. Sensitivity of vertical sky component

The main conclusion of Section 4 is that the Hong Kong sky conditions can be represented by CIE Standard sky types 1, 8, 13 (HKRS) without sacrificing the accuracy of prediction. This section furthers the discussion by examining the influence of HKRS on estimating vertical sky component (VSC).

For the purpose of simplicity, the discussion regarding vertical sky component refers to unobstructed windows facing four cardinal directions.

VSC is the measure of sky light incident on a vertical plane and is a good indication of potential good daylighting. VSC is defined as the ratio of the vertical diffuse illuminance ($E_v$) at a point (usually centre of a window) to the unobstructed horizontal diffuse illuminance available ($E_h$) at the same point on a horizontal plane. In mathematical form it is written as

$$\mathrm{VSC} = E_v/E_h. \tag{2}$$

At present VSC is normally calculated using the CIE Standard Overcast Sky (Sky 1 in Table 1) for building and system designs by designers and engineers. The architectural implications of the new sky proposed can be demonstrated by comparing VSC calculated based on the CIE Standard Overcast Sky model and HKRS, the proposed set of sky types.

### *5.1. Calculating VSC*

The calculation of VSC requires two main steps: calculation of the amount of vertical and horizontal illuminance, respectively.

*Step 1*: Calculating the vertical illuminance.

For an unobstructed window surface, the amount of daylight is mainly determined by luminance from the sky. Furthermore, the area of sky visible through a window has the most significant influence on the internal light. Eq. (3) describes the contribution to the illuminance on a point on a surface from a small patch of sky.

$$\Delta E_{vp} = D_p L_p \Delta S_p, \tag{3}$$

where $D_p$ is the daylight coefficient which in this case (an unobstructed window) depends only on the geometry of the window, $L_p$ the luminance of the sky patch at altitude $\alpha_p$ and azimuth $\phi_p$ and $S_p$ is the angular size of the sky patch.

Please note that under "normal" circumstances (obstructed windows) the daylight coefficient depends on many other factors, such as the surrounding buildings and the reflectance for many surfaces etc. The daylight coefficient ($D_p$) for an unobstructed vertical surface facing azimuth $\phi_v$ is given by

$$D_p = \begin{cases} \cos\alpha_p \cos(\phi_p - \phi_v) & \text{when } 0 \leqslant \alpha_p \leqslant \pi/2,\ -\pi/2 \leqslant (\phi_p - \phi_v) \leqslant \pi/2, \\ 0 & \text{otherwise.} \end{cases} \tag{4}$$

The total diffuse illuminance on a point on a surface is determined by adding the contribution of each patch. Therefore,

$$E_v = \sum_{p=1}^{145} \Delta E_{vp}. \tag{5}$$

*Step 2*: Calculating the horizontal illuminance

The calculation of horizontal illuminance is based on the method outlined in Tregenza [5]. The horizontal illuminance from patch $p$ is given by

$$E_{hp} = \begin{cases} \frac{\pi L_p}{n_p}\left(\sin^2\left(\frac{b_p\pi}{15}\right)\sin^2\left(\frac{(b_p-1)\pi}{15}\right)\right) & \text{when } 1 \leqslant b_p \leqslant 7, \\ \pi\left(1-\sin^2\left(\frac{7\pi}{15}\right)\right) & \text{when } b_p = 8, \end{cases} \tag{6}$$

where $b_p$ is the band containing patch $p$ and $n_p$ the number of patches in band $b_p$.

The total horizontal illuminance is given by

$$E_h = \frac{S_d}{2\pi}\sum_{p=1}^{145} E_{hp}, \tag{7}$$

where

$$S_d = \sum_{p=1}^{145}\left(\sin\left(\frac{b_p\pi}{15}\right) - \sin\left(\frac{(b_p-1)\pi}{15}\right)\right)\left(\frac{2\pi}{n_p}\right). \tag{8}$$

### *5.2. VSC results*

Table 4 shows the error observed in the four cardinal directions when VSC is estimated using the representative sky and sky 1 (the overcast sky). When sky 1 is used the error can be in excess of 50% for a surface east or west. As shown in Table 4, the error can be significantly reduced using the new representative sky (HKRS). Thus, this demonstrates the ability of the new representative sky to characterize the sky conditions in Hong Kong. Furthermore, from the architectural perspective more accurate prediction of VSC can result in better daylight modeling.

Table 4
Error analysis based on the representative sky and sky 1

| | East | West | North | South |
|---|---|---|---|---|
| *Representative sky (HKRS)* | | | | |
| RMSE | 0.21 | 0.14 | 0.08 | 0.15 |
| RMSE % | 42 | 32 | 21 | 28 |
| *Sky 1* | | | | |
| RMSE | 0.27 | 0.24 | 0.12 | 0.23 |
| RMSE % | 51 | 52 | 29 | 44 |
| Reduction in error (%) | 18 | 38 | 27 | 36 |

Table 5
Sensitivity of sky types on VSC

| | East | West | North | South |
|---|---|---|---|---|
| *Summer* | | | | |
| $VSC_{annual}$ (Error %) | 42 | 35 | 21 | 15 |
| $VSC_{seasonal}$ (Error %) | 40 | 37 | 26 | 17 |
| *Winter* | | | | |
| $VSC_{annual}$ (Error %) | 45 | 30 | 22 | 34 |
| $VSC_{seasonal}$ (Error %) | 45 | 30 | 22 | 33 |

### 5.2.1. Seasonal sky types and VSC

The representative sky used for Table 4 utilizes annual frequency distributions of sky types as shown in Fig. 6. It was noted in Table 2 that seasonal sky types can help to reduce the overall error. However, it can be seen in Table 5 that the seasonal sky types do not have a positive influence on predicting VSC. (Remark: In Table 5, $VSC_{annual}$ and $VSC_{seasonal}$ refer to model using annual and seasonal sky types, respectively).

For winter, the results are not surprising as the frequency distribution of sky types does not differ from that of the annual data as shown in Table 3. However, surprisingly VSC based on the summer sky type distribution generally provides worse results than the one based on the annual data. The authors believe that this can be understood by comparing the distribution of VSC under $VSC_{annual}$ and $VSC_{seasonal}$ with the observed VSC distribution. Table 6 was constructed for this purpose using only the summer data. It divides VSC in four different ranges ($0 \leqslant VSC \leqslant 0.4$, $0.4 < VSC \leqslant 0.8$, $0.8 < VSC \leqslant 1$, $1 < VSC \leqslant 1.2$) and calculates frequency (%) for each range. For example the table shows the value of 46% for "$VSC_{annual}$" for "VSC range" of $0 \leqslant VSC \leqslant 0.4$, which means 46% of the all VSC values for the model "$VSC_{annual}$" (i.e. the model based on annual sky type distribution) are between 0 and 0.4.

It is clear from the table that the underlying distribution of VSC is captured very well by $VSC_{annual}$ model, the model based on the annual frequency of sky types. The model based on $VSC_{seasonal}$, using the seasonal sky type (summer, in this case), is only effective for a surface facing east and this is also reflected in Table 5. Therefore, it can be concluded seasonal analysis do not provide any further insights than the annual sky type distribution.

Table 6
Comparing the distribution of VSC based $VSC_{annual}$ and $VSC_{seasona}$ with the observed data (for summer data)

| | VSC distribution | | | |
|---|---|---|---|---|
| | $0 \leqslant VSC \leqslant 0.4$ | $0.4 < VSC \leqslant 0.8$ | $0.8 < VSC \leqslant 1$ | $1 < VSC \leqslant 1.2$ |
| *East* | | | | |
| Observed (%) | 43 | 46 | 7 | 4 |
| $VSC_{annual}$ (%) | 46 | 35 | 12 | 7 |
| $VSC_{seasonal}$ (%) | 49 | 48 | 3 | 0 |
| *West* | | | | |
| Observed (%) | 59 | 34 | 5 | 3 |
| $VSC_{annual}$ (%) | 63 | 27 | 8 | 2 |
| $VSC_{seasonal}$ (%) | 67 | 33 | 0 | 0 |
| *North* | | | | |
| Observed (%) | 49 | 50 | 1 | 0 |
| $VSC_{annual}$ (%) | 56 | 44 | 0 | 0 |
| $VSC_{seasonal}$ (%) | 60 | 40 | 0 | 0 |
| *South* | | | | |
| Observed (%) | 39 | 59 | 2 | 0 |
| $VSC_{annual}$ (%) | 36 | 64 | 0 | 0 |
| $VSC_{seasonal}$ (%) | 70 | 30 | 0 | 0 |

### 5.3. Discussions on VSC

This section discusses the ability of the HKRS based VSC to track the observed VSC. Fig. 9 shows a plot of VSC against time for a surface facing East and the observed data is that for the 14 December 2003 and 15 December 2003. It is interesting to note the characteristic of VSC, calculated using the HKRS, to track the observed VSC. It should be noted that these days are "clear sky days". This is supported by Fig. 10.

Unfortunately, the ability of HKRS based VSC to follow the observed VSC is not applicable to overcast sky days. Fig. 11 shows plots of illuminance for 26 June 2003 and 27 June 2003. These plots clearly confirm that the above 2 days can be classified as "cloudy days". This is because the direct normal illuminance ($E_{vs}$) is almost always approximately zero and the global horizontal illuminance ($E_{vg}$) is primarily dominated by horizontal diffuse illuminance ($E_{vd}$). Under these conditions, HKRS based VSC does not show good agreement with the observed VSC, as shown in Fig. 12.

Figs. 13(a) and (b) reveal that 24 May 2003 and 25 May 2003 are good examples of partially cloudy days. Under partially cloudy conditions, as can be

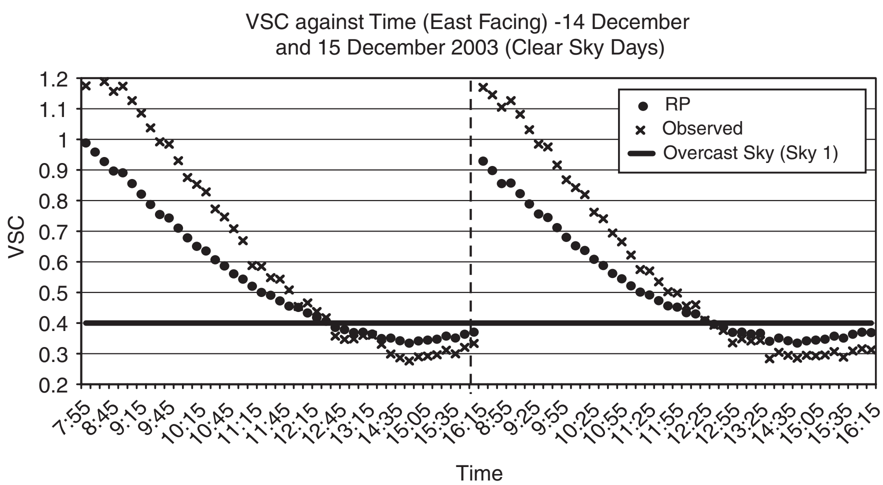


Fig. 9. Plot of VSC against time (East Facing)—14 December 2003 and 15 December 2003.

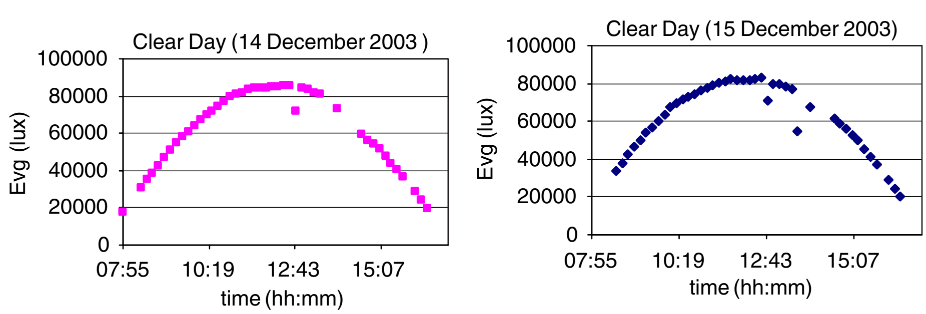


Fig. 10. Plots of $E_{vg}$ against time—14 December 2003 and 15 December 2003.

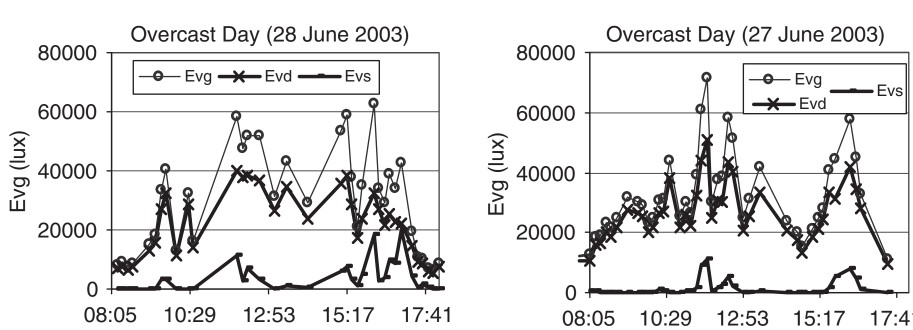


Fig. 11. Plots of illuminance—28 June 2003 and 27 June 2003 (Cloudy Days).

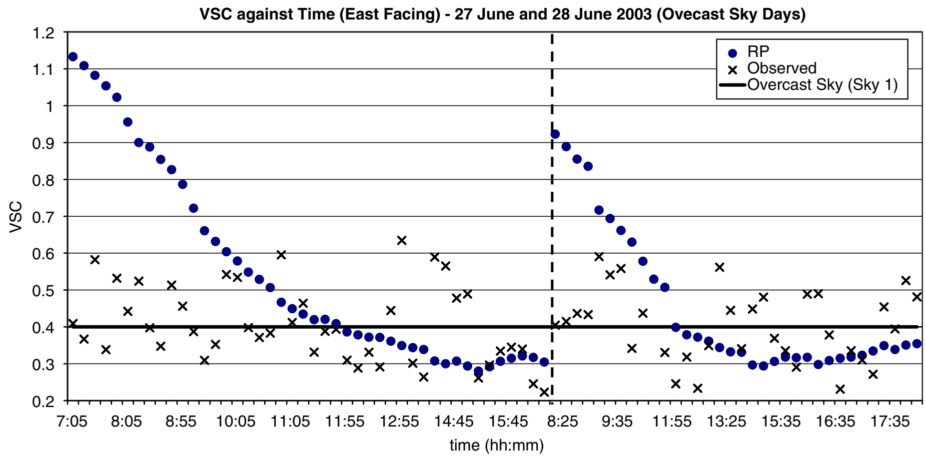


Fig. 12. Plot of VSC against time (East Facing)—27 June and 28 June 2003.

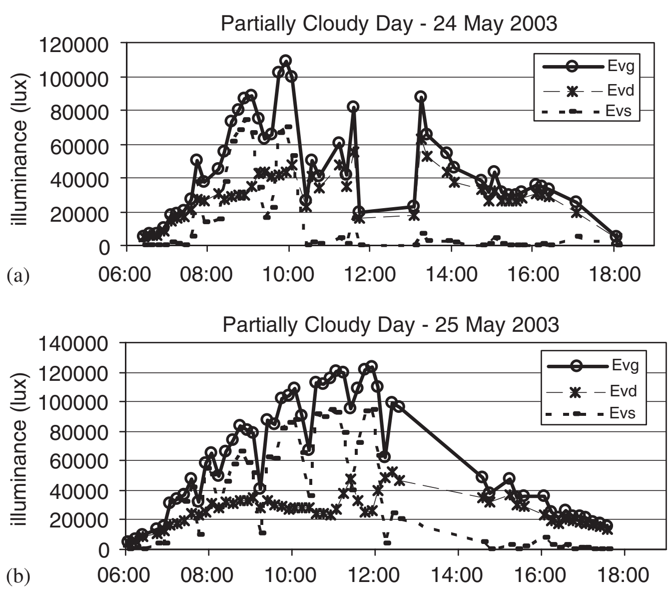


Fig. 13. (a) Partially Cloud Days—24 May 2003, (b) Partially Cloud Days—25 May 2003.

seen in Fig. 14, the HKRS based VSC provides reasonable predictions. However, this does not match the performance under the "clear sky" conditions as shown in Fig. 9.

The inability of the model to cope with different sky conditions is due to generic rigidity in the model. The main flaw is that the sky type probabilities, as shown in Figs. 6(a) and (b), are assumed to be constant for the whole year. If daily probabilities of the proposed sky type set (sky 1, sky 8 and sky 13) are used instead of static probabilities, then perhaps a better fit can be obtained. The authors believe that it is possible to correlate the HKRS to the Hong Kong Observatory's daily weather forecast and this can lead to estimating daily probabilities of the HKRS. The research on the topic is ongoing and will be presented in the paper following this.

## 6. Conclusion

The paper presents results of the IDMP Research Class Station at the Chinese University of Hong Kong. The data was subjected to quality control using CIE Guide to Daylight Measurement (CIE Guideline, (CIE 108-1994), [1]). The main objective of the paper was to establish standard sky types for Hong Kong (HKRS) based on the CIE General Sky type definitions. This subset consists of three sky types, namely this includes CIE General Sky type 1, 8 and 13, representing overcast, intermediate and clear sky, respectively. The annual HKRS, which is based on all of the data, could be characterised by

$$\text{HKRS} = 0.41(\text{sky } 1) + 0.37(\text{sky } 8) + 0.22(\text{sky } 13). \quad (9)$$

Further, the paper evaluated the sensitivity of VSC to differences between the HKRS and the standard CIE Overcast Sky model. By comparing with the observed VSC, it has been shown that, overall speaking, HKRS could give better results. A reduction in error of approximately 20–40% could be expected, depending on the orientation of a surface.

Also, it was found that there is a significant difference in sky types when the yearly analysis is compared to the seasonal analysis. In summer, the HKRS consists of sky types 1, 4 and 8, while in winter it consists of sky types 1, 8 and 13. However, when seasonal sky types were used to estimate VSC very little or no improvement was observed over the yearly sky types, and therefore it was concluded that seasonal analysis does not serve this practical purpose.

The paper also analysed the ability of the HKRS based VSC to track the observed VSC. The HKRS based VSC shows good agreement with the observed VSC for clear sky days, fair results for intermediate days, and

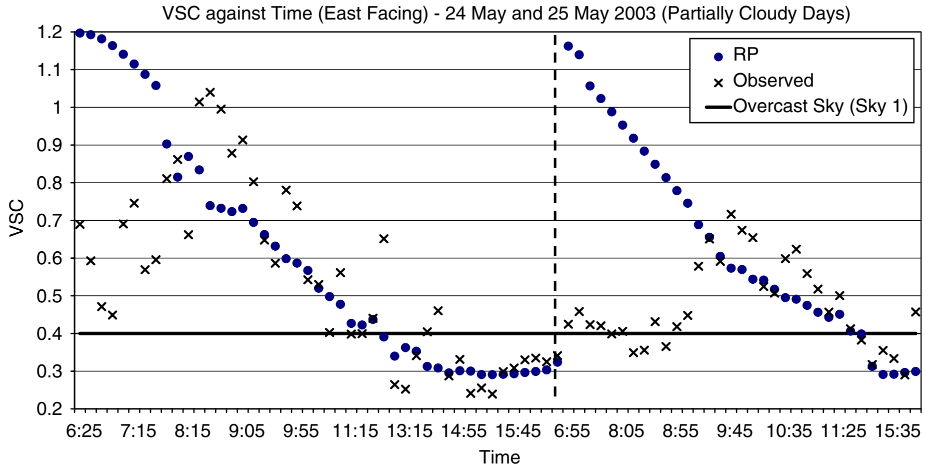


Fig. 14. Plot of VSC against time (East Facing)—24 May 2003 and 25 May 2003.

very poor agreement for overcast days. The authors believe that the generic rigidity of the model is to blame for the inability of the model to cope with different sky conditions. This issue can be addressed by using daily probabilities for HKRS and this will be the key focus of the paper following this.

## References

[1] CIE—Commission Internationale de I'Eclairage. CIE Guideline (CIE 108-1994) Guide to recommended practice of daylight measurement, CIE Vienna, 1994.

[2] Boyce PR. Human factors in lighting. 2nd ed. London: Taylor & Francis; 2003.

[3] Compte Rendu, CIE 12 Session 1955. Natural Daylight. Official Recommendation, 2, part 3.2, II-IV & 35-37 (1955).

[4] Tregenza PR. Standard skies for maritime climates. Lighting Research and Technology 1999;31(3):97–106.

[5] Tregenza PR. Analysing sky luminance scans to obtain frequency distributions of CIE Standard General Skies. Lighting Research and Technology 2004;36(4):271–81.

[6] CIE—Commission Internationale de I'Eclairage. CIE Standard (CIE S 011/E:2003) Spatial distribution of daylight—CIE standard general sky, CIE Vienna, 2003.

[7] Li DHW, et al. A study of 15 sky luminance patterns against Hong Kong data. Architectural Science Review 2003;46(1):61–8.